

## Strut-and-Tie Models for the Design of Pile Caps: An Experimental Study



by Perry Adebar, Daniel Kuchma, and Michael P. Collins

*Describes the test results from six large pile caps that failed in two-way shear. ACI Building Code procedures for the shear design of pile caps are unable to predict the experimental results because the procedures neglect certain important parameters, such as the amount of longitudinal reinforcement, and overemphasize other parameters, such as the effective depth. Strut-and-tie models were found to describe more accurately the behavior of deep pile caps.*

**Keywords:** building codes; caps (supports); deep beams; footings; piles; reinforced concrete; shear strength; structural design; tests.

A pile cap is a structural member whose function is to transfer load from a column to a group of piles [see Fig. 1(a)]. Current design procedures for pile caps do not provide engineers with a clear understanding of the physical behavior of these elements. Strut-and-tie models, on the other hand, can provide this understanding and hence offer the possibility of improving current design practice.

The design procedure for pile caps given in the ACI Building Code (ACI 318-83) is a "sectional force" approach similar to that used for two-way slabs. The procedure is divided into two separate steps: (1) shear design, which involves calculating the minimum pile-cap depth so that the concrete contribution to shear resistance is greater than the shear applied on the defined pseudocritical section; and (2) flexural design, in which the usual assumptions for reinforced concrete beams are used to determine the required amount of longitudinal reinforcement.

Strut-and-tie models consider the complete flow of forces within the structure rather than just the forces at one particular section. The internal load path in cracked reinforced concrete is approximated by an idealized truss [see Fig. 1(b)]. Zones of concrete with primarily unidirectional compressive stresses are modeled by compression struts, while tension ties are used to model the principal reinforcement. The areas of concrete where struts and ties meet, referred to as nodal zones, are analogous to the joints of a truss (see Fig. 2). While truss models have been used in reinforced con-

crete design since the turn of the century, recent work has refined and improved these models.<sup>1,4</sup>

A simple design procedure that uses strut-and-tie models forms part of the new shear design provisions of CAN3 A23.3-M84, the Canadian concrete code.<sup>5,6</sup> The procedure is used for regions near statical or geometrical discontinuities where it is inappropriate to assume that shear stresses are uniformly distributed over the depth of the member. In addition to the usual equilibrium conditions of strut-and-tie models, the Canadian code requires some consideration of compatibility conditions.

Many experimental studies have confirmed the suitability of strut-and-tie models for deep beams, e.g., References 7 and 8. Unlike deep beams, pile caps are large blocks of concrete containing little reinforcement. They usually contain no transverse shear reinforcement and only small percentages of longitudinal reinforcement. This paper reports the results of six large pile-cap tests designed to examine the suitability of three-dimensional strut-and-tie models for pile-cap design.

### PREVIOUS TESTS ON PILE CAPS

Blévoit and Frémy<sup>9</sup> conducted a comprehensive series of tests on about 100 pile caps, most of which were half-scale, to investigate the influence of different reinforcement arrangements. In the case of four-pile caps (i.e., pile caps supported on four piles), they found that spreading out the reinforcement uniformly (as suggested by the ACI Building Code) reduced the failure load by 20 percent compared to a pile cap with the same quantity of reinforcement but with all the reinforcement concentrated over the piles (as suggested by

ACI Structural Journal, V. 87, No. 1, January-February 1990.  
Received Jan. 5, 1989, and reviewed under Institute publication policies.  
Copyright © 1990, American Concrete Institute. All rights reserved, including the making of copies unless permission is obtained from the copyright proprietor. Pertinent discussion will be published in the November-December 1990 ACI Structural Journal if received by July 1, 1990.

ACI member Perry Adebar is a doctoral candidate in the Department of Civil Engineering at the University of Toronto. He holds engineering degrees from Lakehead University and the University of Toronto.

Daniel Kuchma is a doctoral candidate in the Department of Civil Engineering at the University of Toronto.

Michael P. Collins, FACI, is a professor in the Department of Civil Engineering at the University of Toronto. He is a member of Joint ACI-ASCE Committee 445, Shear and Torsion; and of ACI Committees 358, Concrete Guideways, and E901, Scholarships; and of Subcommittee 318E, Shear and Torsion. He has acted as a consultant on the shear design of Condeep concrete offshore platforms.

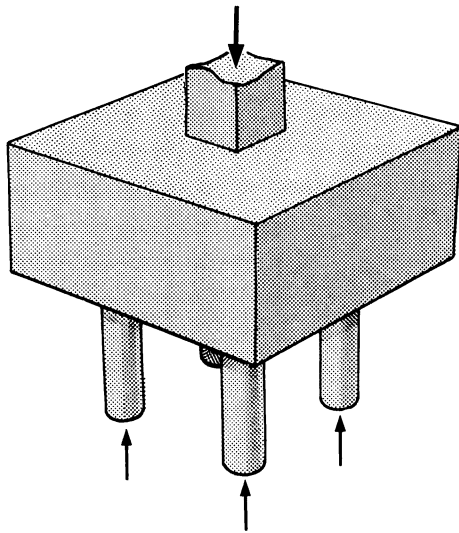


Fig. 1(a)—Pile cap supported on four piles

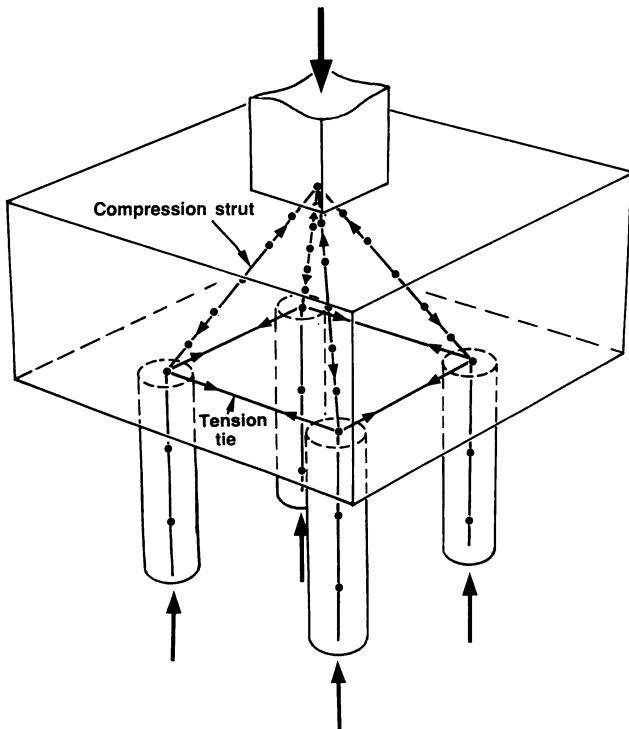


Fig. 1(b)—Simple three-dimensional truss model for a four-pile cap

strut-and-tie models). For three-pile caps, spreading the reinforcement uniformly across the width caused a 50-percent reduction in strength.

Clarke<sup>10</sup> tested 15 four-pile caps at one-half scale to study the influence of reinforcing-steel layout and reinforcing-bar anchorage. He found that spreading the reinforcement out uniformly reduced the failure load by 14 percent. For pile caps with reinforcement concentrated over the piles, Clarke observed that the anchorage of reinforcing bars was enhanced by the confining action of the compression struts.

Sabnis and Gogate<sup>11</sup> recently tested nine four-pile cap models at one-fifth scale with varying amounts of uniformly placed reinforcement. They concluded that the ACI Building Code requires “major revisions to properly reflect the behavior of thick pile caps.”

### PRESENT EXPERIMENTAL STUDY

Details of the six test specimens are given in Fig. 3 and Table 1. Pile Caps A, B, D, and E were all four-pile caps with identical external dimensions. Pile Cap A was designed in accordance with the ACI Building Code (ACI 318-83) for an ultimate column load of about 2000 kN (450 kips). The calculated reinforcement was not increased to satisfy minimum temperature and shrinkage reinforcement requirements. Pile Cap B was designed using a strut-and-tie model for a column load of 2000 kN (450 kips). Pile Cap D was constructed with twice as much reinforcement as Pile Cap B to investigate failure prior to yielding of the reinforcement. Pile Cap E was similar to Pile Cap D, except it contained distributed reinforcement.

Pile Cap C was supported on six piles and was designed using a strut-and-tie model for a 3000-kN (675-kip) load.

Pile Cap F was constructed to test a hypothesis of the ACI Building Code. It was made identical to Pile Cap

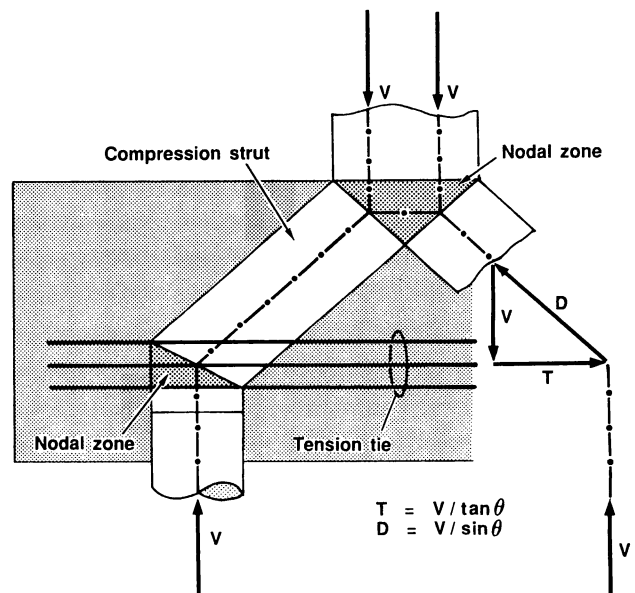


Fig. 2—Components of the idealized load-resisting truss

D except that four "corner" pieces of plain concrete were omitted (see Fig. 3). Because of these missing pieces of concrete, the ACI Building Code predicts that Pile Cap F will have a much lower strength than Pile Cap D. The strut-and-tie model suggests that Pile Caps D and F will have essentially the same strength.

In designing the pile caps, it was assumed that the column load would be equally shared among all the piles, as is the usual assumption in pile-cap design. However, it is important to recognize that the loads in the piles are, in fact, statically indeterminate and are influenced by the relative stiffnesses of the individual piles. In this study, the stiffnesses of the pseudo-piles were not uniform.

The pile caps all had an overall depth of 600 mm (24 in.) and were loaded through 300 mm (12 in.) square cast-in-place reinforced concrete columns. They were supported by 200 mm (8 in.) diameter precast reinforced concrete piles embedded 100 mm (4 in.) into the underside of the pile caps [Fig. 3(b)].

The concrete used to construct the pile caps was obtained from a ready-mix supplier. A compressive strength of 20 MPa (2900 psi) was specified. Results from tests on standard cylinders of the concrete are given in Table 2. Properties of the reinforcing bars are given in Table 3.

**Table 1 — Summary of reinforcement**

Tension tie mark (see Fig. 3)	Reinforcing steel	Area of steel, mm <sup>2</sup>	Depth to centroid, mm
TA1	9-No. 10* at 260 mm	900	440
TA2	15-No. 10 at 100 mm	1500	450
TB1	4-No. 10 at 70 mm	400	340
	4-No. 10 at 70 mm	400	390
	4-No. 10 at 70 mm	400	440
		1200	
TB2	6-No. 10 at 45 mm	800	350
	8-No. 10 at 45 mm	800	400
	8-No. 10 at 45 mm	600	450
		2200	
TC2	3-No. 10 at 45 mm	300	340
	5-No. 10 at 45 mm	500	390
	3-No. 10 at 45 mm	300	440
		1100	
TC3	7-No. 10 at 45 mm	700	350
	7-No. 10 at 45 mm	700	400
	7-No. 10 at 45 mm	700	450
		2100	
TD1	4-No. 15† at 70 mm	800	330
	4-No. 15 at 70 mm	800	380
	4-No. 15 at 70 mm	800	430
		2400	
TD2	8-No. 15 at 45 mm	1600	350
	8-No. 15 at 45 mm	1600	400
	8-No. 15 at 45 mm	1600	450
		4800	
TE3	9-No. 10 at 210 mm	900	495
TE4	5-No. 10 at 240 mm	500	485
TE5	1-No. 10	100	250
	1-No. 10	100	325
	1-No. 15	200	400
	1-No. 15	200	470

\*No. 10 is a 11.3 mm diameter bar with a cross-sectional area of 100 mm<sup>2</sup>.  
 †No. 15 is a 16.0 mm diameter bar with a cross-sectional area of 200 mm<sup>2</sup>.  
 1 mm<sup>2</sup> = 0.015 in.<sup>2</sup>; 1 mm = 0.0394 in.

The total load applied to the pile cap and the load carried by each pile were measured using load cells. Vertical and horizontal deflections of the pile caps were measured with displacement transducers and mechanical dial gages. Electrical-resistance strain gages were in-

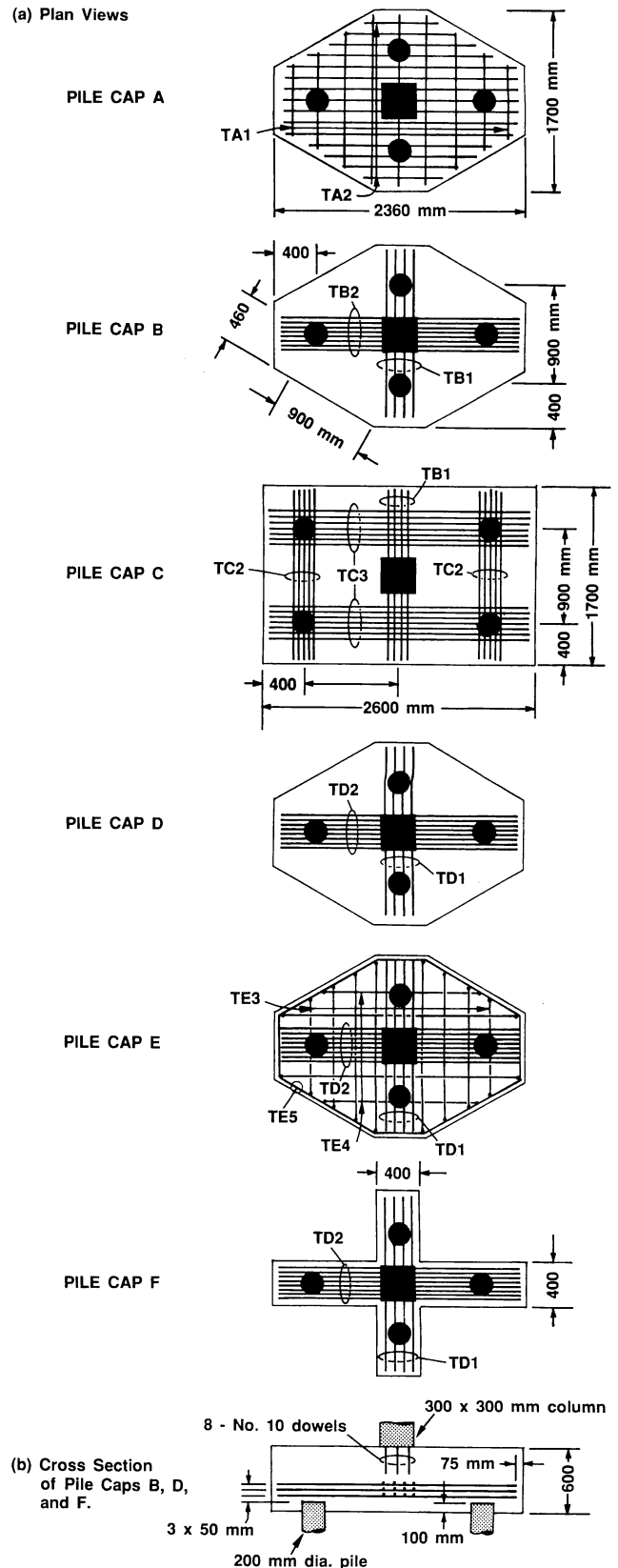


**Fig. 3—Test specimens**

stalled at numerous locations along selected reinforcing bars, and demountable strain gages were used to measure average strains on some surfaces. To determine strains within the large volume of plain concrete, as many as 20 embedment strain gages, with 75 mm (3 in.) gage lengths, were cast into each specimen.

A universal testing frame was used to apply concentric compressive load onto the columns. Short reinforced concrete piles were supported on steel pedestals, which in turn were supported on rubber pads and non-stick synthetic-resin-coated sliding bearings (see Fig. 4). The load on the specimens was increased monotonically to failure, stopping at approximately 10 deformation stages to take manual displacement readings and to photograph crack development. All electronic measurements were automatically recorded during the test by a computerized data acquisition system.

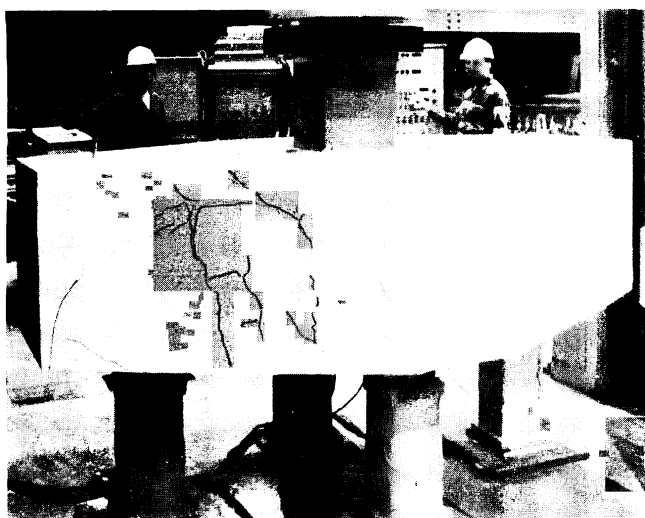


Fig. 4—Pile Cap E being tested

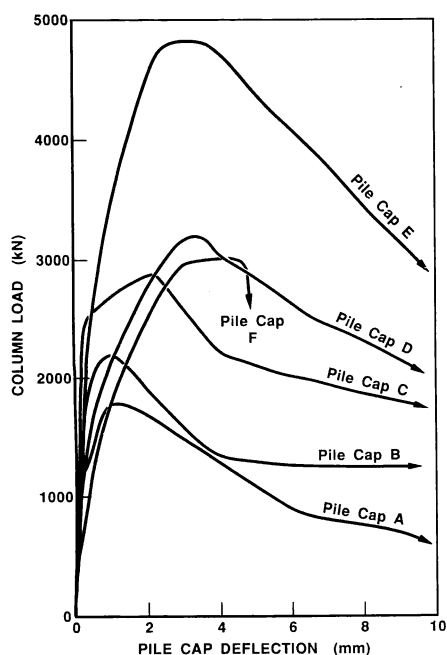


Fig. 5—Load-deflection relationships for the six test specimens (1 kN = 0.225 kips; 1 mm = 0.0394 in.)

## EXPERIMENTAL OBSERVATIONS

The observed load-deflection relationships for the six specimens are shown in Fig. 5. The pile cap center deflection, load distribution among the piles, and reinforcing-bar strains, at both cracking load and ultimate load, are shown in Table 4. In Pile Caps A and B, which were lightly reinforced, the reinforcing strains increased very suddenly when the first crack formed. Both the strains immediately before and immediately after cracking are shown in the table.

The pile caps typically had very few cracks prior to failure. One flexural crack usually occurred in each span between the piles. In the diamond-shaped specimens (Pile Caps A, B, D, and E), the flexural cracks extended diagonally between the piles (see Fig. 6). Failure in all pile caps was characterized by the rapid development of many new cracks.

Pile Cap A was predicted to fail at a total load of 2138 kN (481 kips) by the design equations of the ACI Building Code, with flexure being critical. However, the specimen failed at only 83 percent of this predicted load, namely 1781 kN (401 kips). Fig. 6 shows the deformation pattern at failure. The zones that are shaded in the figure moved down relative to the unshaded zones to produce a typical two-way shear failure cone. The flexural reinforcement yielded prior to failure.

Pile Cap B was similar to Pile Cap A except for the reinforcement, which was designed according to a strut-and-tie model for equal pile loads of 500 kN (112.5 kips), e.g., a 2000 kN (450 kip) total load. The majority of the load was initially carried to the two piles closest to the column. After the tension tie in the short direction yielded, the load distribution among the piles began to change. The specimen failed before significant redistribution occurred. The pile cap resisted a maximum load of 2189 kN (492.5 kips). The tension tie in the long direction did not yield. For the physical appearance of Pile Cap B after testing, see Fig. 7.

Table 2 — Results of concrete cylinder tests

Pile Cap	Cylinder compressive test			Tensile strength from indirect tension tests, MPa	
	Secant modulus,* MPa	Peak stress, MPa	Strain at peak stress	Split cylinder	Double punch <sup>18</sup>
A	19,400	24.8	0.0024	2.9	—
B	19,400	24.8	0.0024	2.9	—
C	26,000	27.1	0.0020	3.7	—
D	28,600	30.3	0.0020	2.2	2.0
E	31,600	41.1	0.0022	2.7	2.5
F	28,600	30.3	0.0020	2.2	2.0

\*Secant modulus measured to a stress of  $0.4 f_c$ .  
1 MPa = 145 psi.

Table 3 — Properties of reinforcing steel

Bar designation	Nominal area, mm <sup>2</sup>	Yield load, kN	Yield stress $f_y$ , MPa	$f_y/E_s$	Ultimate stress, MPa
No. 10M	100	47.9	479	0.0024	610
No. 15M	200	97.2	486	0.0024	646

$E_s$  (Young's modulus of steel) = 200,000 MPa.  
1 mm<sup>2</sup> = 0.0015 in.<sup>2</sup>; 1 kN = 0.225 kip; 1 MPa = 145 psi.

Pile Cap C was designed for six equal pile loads of 500 kN (112.5 kips), i.e., a column load of 3000 kN (675 kips). As in Pile Cap B, the vast majority of the load was resisted by the two piles closest to the column, while the four outer piles resisted very little load. Even though the strain of the tension tie between the center two piles reached the yield strain, very little de-

formation occurred because of the restraint provided by the adjoining portions of the pile cap (see Fig. 3). When the total column load reached 2892 kN (651 kips), a shear failure occurred. A punching cone extended from the column's outside faces to the piles' inside edges (Fig. 8). The two piles closest to the column had maximum individual loads of 1150 kN (259 kips) each.

**Table 4 — Summary of experimental observations**

Pile Cap	Load, kN	Center deflection, mm	Pile load distribution		Reinforcing bar strain		
			Load on closest two piles, kN (percent)	Load on other piles, kN (percent)	Between closest two piles, mm/m	Between other piles, mm/m	
Observations at 1st cracking	A	1186	0.10	676 (57)	510 (43)	0.11 1.34*	0.20 1.10*
	B	1679	0.04	1461 (88)	218 (12)	0.38 1.43*	0.05 0.67*
	C	1780	0.15	1615 (91)	165 (9)	0.11	0.05
	D	1122	0.16	823 (73)	299 (27)	0.06	0.05
	E	1228	0.11	910 (74)	318 (26)	0.01	0.01
	F	650	0.18	474 (73)	176 (27)	0.09	0.20
Observations at failure	A	1781	1.59	1247 (70)	534 (30)	13.0	2.6
	B	2189	1.07	1575 (72)	614 (28)	9.2	1.3
	C	2892	2.06	2303 (80)	589 (20)	2.4	1.0
	D	3222	3.37	2205 (68)	1017 (32)	1.9	1.3
	E	4709	2.50	3243 (69)	1466 (31)	0.8	0.4
	F	3026	3.21	2059 (68)	965 (32)	2.2	1.1

\*Strain immediately after cracking.  
1 kN = 0.225 kip; 1 mm = 0.0394 in.

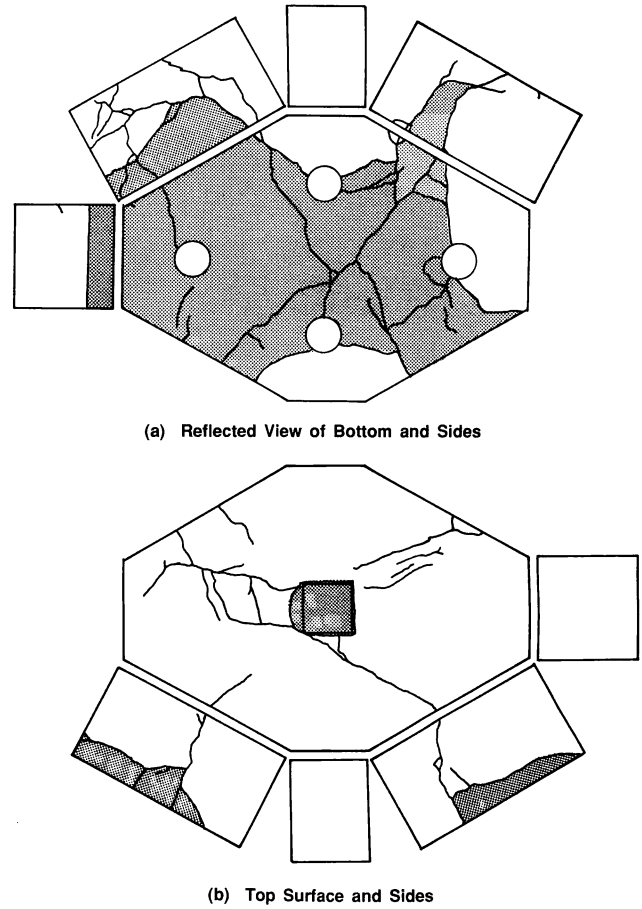


**Fig. 6—Final deformation pattern of Pile Cap A**

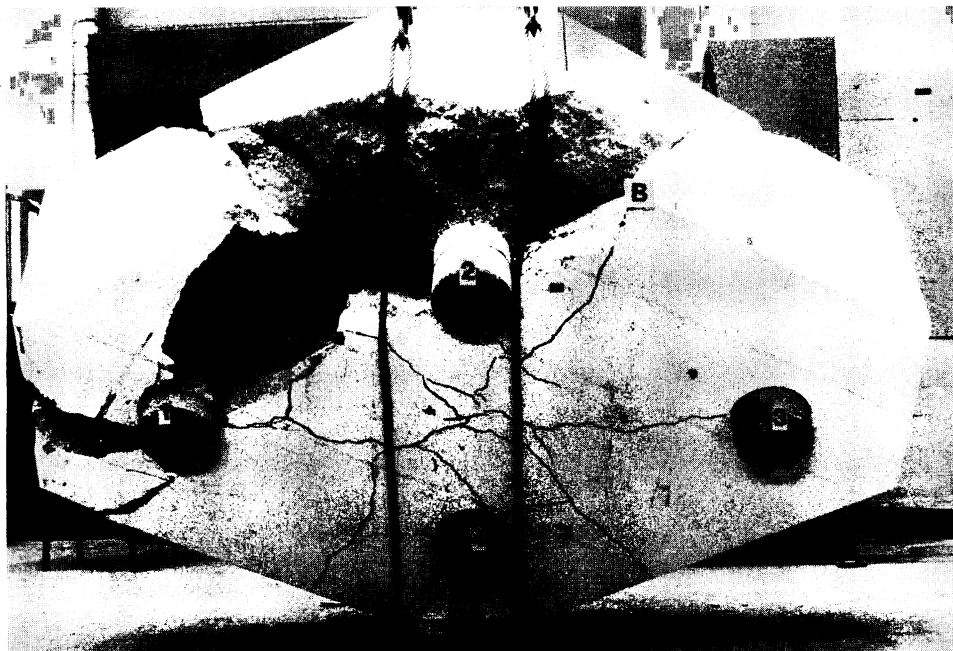


**Fig. 7—Appearance of Pile Cap B after testing**



Fig. 8—A view of the punching cone in Pile Cap C after part of the specimen was removed

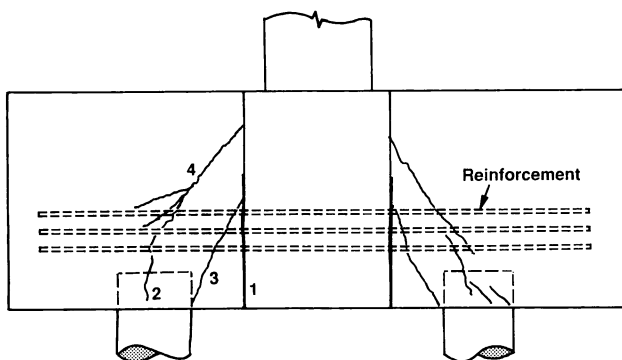


Fig. 9(a)—Sequence of relevant crack formations in Pile Cap F



Fig. 9(b)—Appearance of failure zone in Pile Cap F after testing

Pile Caps D and E, which were similar to Pile Cap B except that they had twice as much reinforcement, both failed prior to yielding of either tension tie. Once again the failure surfaces resembled typical punching shear cones. Pile Cap D failed at a column load of 3222 kN (735 kips) with a maximum individual pile load of 1119 kN (252 kips). Pile Cap E failed when the column load was 2709 kN (1060 kips) and the maximum individual pile load was 1655 kN (372 kips). Pile Cap E was stronger than Pile Cap D because of the distributed reinforcement in that specimen and also the higher concrete strength.

Pile Cap F was similar to Pile Cap D except for the four “missing corners” of plain concrete. The specimen resembled two orthogonal deep beams intersecting at midspan. Failure occurred when the short beam failed in shear. The sequence of relevant crack formations in the shorter span beam is illustrated in Fig. 9(a). The first cracks to form were flexural cracks at midspan, which propagated up the interface of the two beams labeled 1 in Fig. 9(a). A vertical crack, labeled 2, then appeared directly above the pile. At a pile load of 949 kN (214 kips), a new diagonal crack suddenly appeared (Crack 4). Analogous to a web-shear crack, this diagonal crack formed independently of any previously existing cracks. With a small increase in load, the diagonal crack widened considerably. The specimen failed when the shear in the short beam, i.e., the short-direction pile load, was 1077 kN (242 kips) and the total column load was 3026 kN (681 kips). None of the longitudinal reinforcement yielded. The appearance of the failure zone can be seen in Fig. 9(b).

More detailed experimental observations are reported in References 12 and 13.

The ACI Building Code suggests that the usual procedures for flexural design be applied in designing the longitudinal reinforcement in a pile cap. Fundamental to these “beam” procedures is the assumption that plane sections remain plane. To investigate the validity

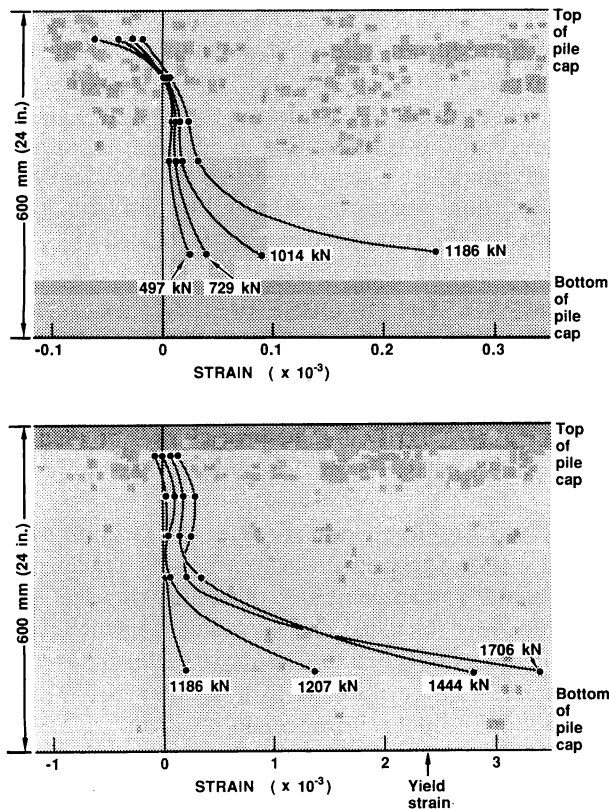
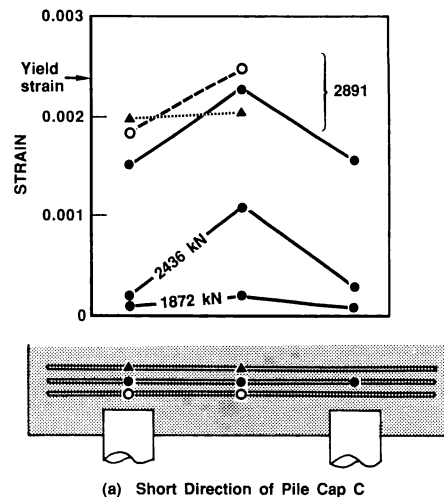


Fig. 10—Measured vertical strain profiles in long direction of Pile Cap A at various column loads (1 kN = 0.225 kips)

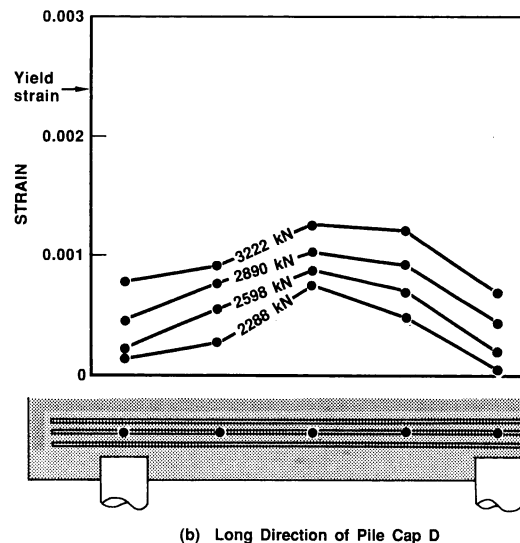
of this assumption, the variation of horizontal strain over the depth of the pile caps was measured directly beneath the column. Both embedment strain gages in concrete and strain gages on reinforcing bars were used.

The ACI Building Code states that a nonlinear distribution of strain need not be considered if the overall depth-to-clear span ratio is less than 0.8 for simply supported members. Fig. 10 shows the measured strain profiles in the long direction of Pile Cap A at various load stages. The overall depth-to-clear span ratio for this case is about 0.4. However, it can be seen that the strain distributions are highly nonlinear both prior to cracking at a load of 1186 kN (267 kips) and after cracking.

In a member that resists shear by true “beam action,” the tension force in the longitudinal reinforcement changes along the beam to balance the applied bending moment, while the flexural lever arm remains relatively constant.<sup>14</sup> Alternatively, if the tension force remains constant, the flexural lever arm changes and the member acts as a tied arch with the shear being resisted by inclined compression, i.e., “strut action.” Fig. 11 shows typical examples of longitudinal reinforcing strain variations measured in the pile caps. While the sectional bending moment varies linearly from maximum at midspan to zero at the piles, the tensile force in the reinforcement varies much less. The measured tension in the reinforcement had its highest value at midspan, but the reinforcement over the piles still carried up to 75 percent of this maximum tension. It is perhaps the main advantage of strut-and-tie models



(a) Short Direction of Pile Cap C



(b) Long Direction of Pile Cap D

Fig. 11—Typical examples of longitudinal reinforcing strain variations measured at various column loads (1 kN = 0.225 kips)

that they clearly indicate to the designer the need to anchor the longitudinal reinforcement so that it can develop this high tension force at the piles.

Another important assumption in the ACI Building Code “beam method” of pile-cap design is that the full width of the pile cap uniformly resists the applied bending moment. To investigate this assumption, longitudinal strains on the top surfaces of the pile caps were measured across the widths of the pile caps. The observed strain profiles for Pile Cap A at a column load of 1706 kN (384 kips) are shown in Fig. 12. Even though the flexural reinforcement was yielding and the pile cap was very close to failure, the compressive strains on the top surface remained relatively low. Also, the surface strains were far from uniform, indicating that the bending moment was resisted mainly by the central portion of the pile cap, as suggested by the strut-and-tie model.

To gather more information on the zones of concrete that resist the load, an array of embedment strain gages was installed in Pile Cap A and Pile Cap B [see Fig. 13(a)]. Note that the embedment gages measured the

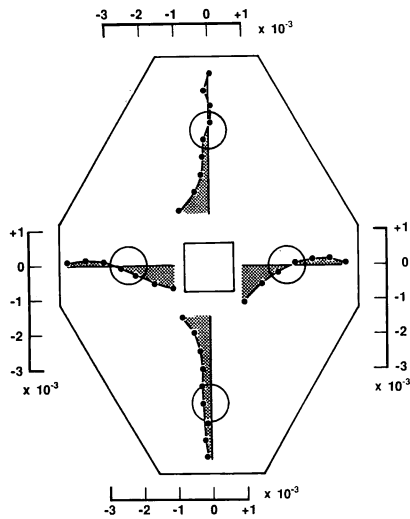
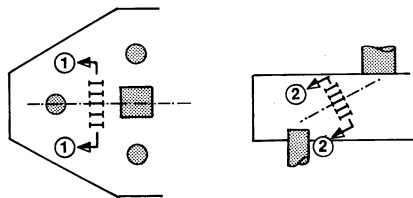
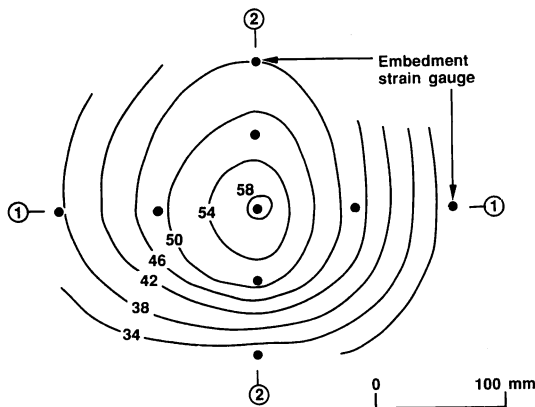


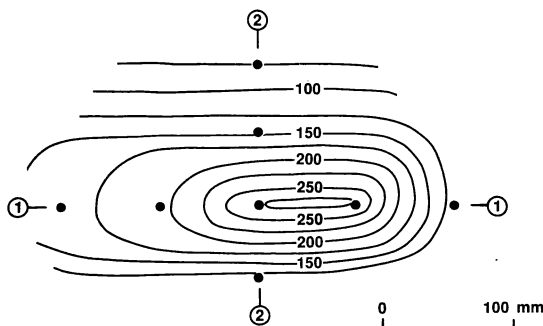
Fig. 12—Longitudinal strains on top surface of Pile Cap A at approximate failure, i.e., column load of 1706 kN (384 kips)



(a) Location of Embedment Strain Gauges



(b) Compressive Strain Contours in Pile Cap A at Failure  
Numbers shown are microstrain, i.e.  $\times 10^{-6}$



(c) Compressive Strain Contours in Pile Cap B at Failure  
Numbers shown are microstrain, i.e.  $\times 10^{-6}$

Fig. 13—Contours of compressive strain in zones of concrete that resist load

compressive strains in the struts joining the column to the two more distant piles, but the majority of the load was traveling to the closer piles. The measured strains were used to draw the strain contours shown in Fig. 13(b) and 13(c). It is interesting to note that in both pile caps the compressive strains reached their highest value at the location where the strut-and-tie model suggests the center of the compression strut is located.

### COMPARISON OF OBSERVED STRENGTHS WITH ACI BUILDING CODE PREDICTIONS

The requirements for the design of footings, including those supported on piles, are given in Chapter 15, Footings, of ACI 318-83. The procedure is divided into two separate parts, design for moment and design for shear.

The ACI Building Code specifies the location of the critical section for moment in footings. The quantity of longitudinal reinforcement required at this section is determined by the usual procedures for reinforced concrete members outlined in Chapter 10, Flexure and Axial Loads. The designer is told to distribute the required longitudinal reinforcement uniformly across the footing (except that the short-direction reinforcement of rectangular footings must be somewhat more concentrated near the center of the pile cap).

The shear strength of footings is required to be in accordance with Section 11.11, Special Provisions for Slabs and Footings. The shear strength of slabs and footings is said to be governed by the more severe of two conditions: beam action, where the footing is considered to be acting as a wide beam; and two-way action, where failure occurs by punching along a truncated cone. In the first case the critical section is a plane located  $d$  from the face of the column, whereas in the second case the critical surface is at  $d/2$  from the perimeter of the column. In calculating the shear in a footing, any pile located inside the critical section is considered to produce no shear according to Paragraph 15.5.3.

The procedures of the ACI Building Code were used to predict the failure loads of the test specimens (see Table 5). Pile Cap A was predicted to fail in flexure, while all other specimens were predicted to fail in shear. All specimens, including Pile Cap A, actually failed in shear.

Pile Cap A, the specimen designed according to the ACI Building Code, failed in two-way shear at 83 percent of the predicted load. The low strength of this specimen was due to yielding of the longitudinal reinforcement in the short direction that triggered a punching shear failure.

The predicted two-way shear strength of Pile Cap A is 2366 kN (528 kips), 29 percent greater than the predicted two-way shear strength of Pile Cap B. The difference is large because the predictions are very sensitive to the effective depth  $d$ . Pile Cap A had one layer of longitudinal reinforcement, while Pile Cap B had three layers, resulting in a smaller effective depth to the centroid of the reinforcement. The experimental results



**Table 5 — Comparison of ACI predictions and experimentally observed failure loads**

Pile Cap	Concrete strength $f'_c$ , MPa	ACI predicted failure loads, kN		Experimental load, kN	Exp. Pred.
		Flexure	Shear		
A	24.8	2138	2366	1781	0.83
B	24.8	2778	1833	2189	1.19
C	27.1	4086	1898	2892	1.52
D	30.3	5645	1966	3222	1.64
E	41.1	7404	2451	4709	1.92
F	30.3	5187	1204	3026	2.51

Mean = 1.60  
Coefficient of variation = 36.4%

1 MPa = 145 psi; 1 kN = 0.225 kip.

were actually opposite to those that had been predicted: Pile Cap B was in reality 23 percent stronger than Pile Cap A.

The strong influence of amount of longitudinal reinforcement can be seen if Pile Cap B is compared with Pile Cap D. The ACI Building Code predicts that Pile Cap D should only be 7 percent stronger than Pile Cap B because of its higher concrete strength. Pile Cap D, which contained twice as much longitudinal reinforcement, was in fact 47 percent stronger than Pile Cap B. The ACI Building Code expressions for two-way shear strength are independent of the amount of longitudinal reinforcement.

Pile Caps D and F were identical except that four "corner" pieces of plain concrete were omitted in Pile Cap F. Because of these missing pieces of concrete, the ACI Building Code expressions predict that Pile Cap D will be 63 percent stronger than Pile Cap F. This great difference in predicted strength results from the fact that Pile Cap D is predicted to fail in two-way shear, while Pile Cap F is predicted to fail in one-way shear (see Fig. 14). The strut-and-tie model suggests that concentrated zones of concrete (compression struts) transmit the load and that failure occurs when the stress in a compression strut reaches some critical value. The strut-and-tie model predicts little difference between the strengths of Pile Caps D and F, which had identical concrete strengths. The failure loads of the two specimens actually differed by less than 7 percent.

### FAILURE OF COMPRESSION STRUTS

If a tension tie crosses a compression strut, the required tensile straining can reduce the capacity of the concrete to resist compressive stress.<sup>15</sup> In pile caps, tension ties cross compression struts in the vicinity of the nodal zones just above the piles. For four of the pile caps tested, the average biaxial strains of these critical regions were measured using two embedment strain gages in the concrete and one strain gage on a reinforcing bar at each location. See Fig. 15. The measured biaxial strains are presented in Table 6 in terms of principal strains. For Pile Cap C, the strains are shown at increasing load levels from before cracking up to failure. Also, for the three other specimens, the strains at failure are presented. In none of the pile caps did the principal compressive strain reach very high values.

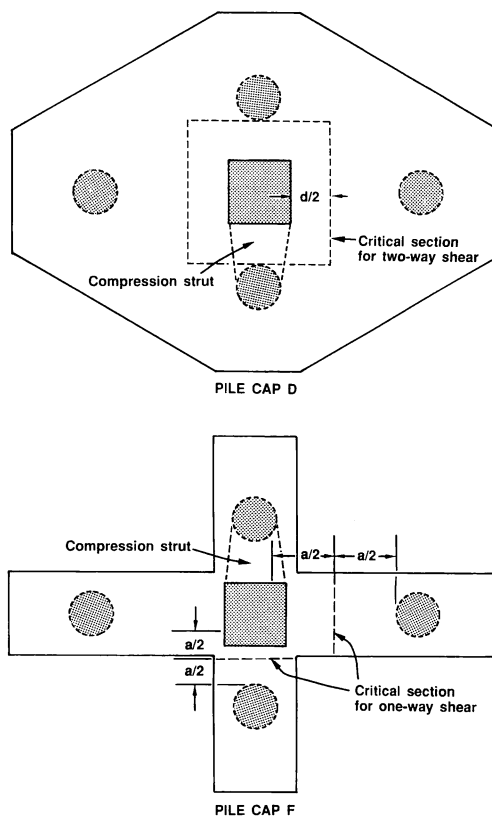


*Fig. 14—ACI Building Code critical sections for shear capacity in Pile Cap D and Pile Cap F*

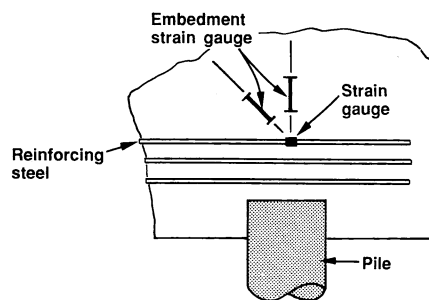


*Fig. 15—Internal biaxial strain measurements*

Further, the principal tensile strains remained relatively small. These strain values indicate the compression struts did not fail by crushing of the concrete.

The strut-and-tie model shown in Fig. 2 is a very simple idealization of force flow. More refined strut-and-tie models can be developed by considering the flow of elastic stresses.<sup>1</sup> Since pile caps remain virtually uncracked until failure, the linear elastic stress distributions are especially relevant. Fig. 16(a) shows the biaxial stress trajectories determined from a linear elastic finite element study. Note that between the points of load application, the compressive stresses spread out, producing transverse tensile stresses. A refined truss model, which includes a concrete tension tie to resist the transverse tension, is shown in Fig. 16(b). It is believed that failure of this concrete tension tie was the critical mechanism involved in the shear failures of the pile caps tested.

**Table 6 — Average biaxial strains at intersections of compression struts and tension ties**

Pile Cap	Load, kN	$\epsilon_1$ , $\times 10^{-3}$	$\epsilon_2$ , $\times 10^{-3}$	$\theta_2$ , deg*
C	1007	0.07	-0.05	57.5
	1513	0.11	-0.08	58.0
	2006	0.16	-0.11	58.8
	2312	0.21	-0.14	59.8
	2591	0.66	-0.30	60.9
	2607	1.20	-0.40	62.9
	2752	1.78	-0.52	63.8
	2891	2.66	-0.69	64.6
D	3222	2.33	-1.20	57.3
E	4709	0.66	-0.28	64.7
F	3026	1.97	-0.89	57.6

\* $\theta_2$  is measured from horizontal.  
1 kN = 0.225 kip.

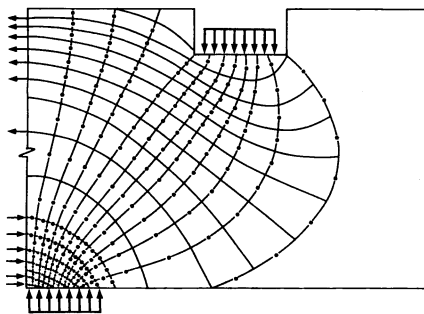


**Fig. 16(a)—Linear elastic stress trajectories showing transverse tensioning due to spreading of compression in Pile Cap F**

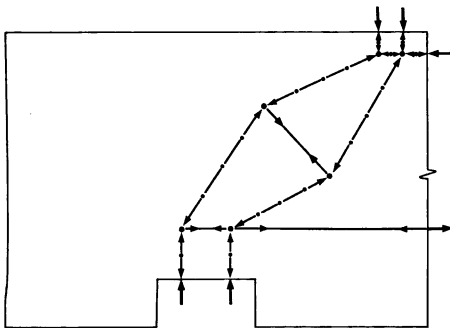


**Fig. 16(b)—Refined truss model that includes a concrete tension tie to resist transverse tension**

Rather than employing a refined strut-and-tie model, the simple truss model combined with an appropriate failure criterion for the compression strut can be used.<sup>1</sup> Fig. 17 summarizes a series of simple tests conducted by the authors to demonstrate the influence of transverse tension on the failure of compression struts. Seven plain concrete specimens with constant height and thickness but with varying widths were loaded in uniaxial compression, using the same size loading plate in all cases. In all but the most narrow specimen, the compression spread out, causing transverse tension, which split the specimens. The measured cracking loads, expressed in terms of the bearing stress, are compared with an elastic finite element prediction. In making this prediction, cracking was assumed to occur

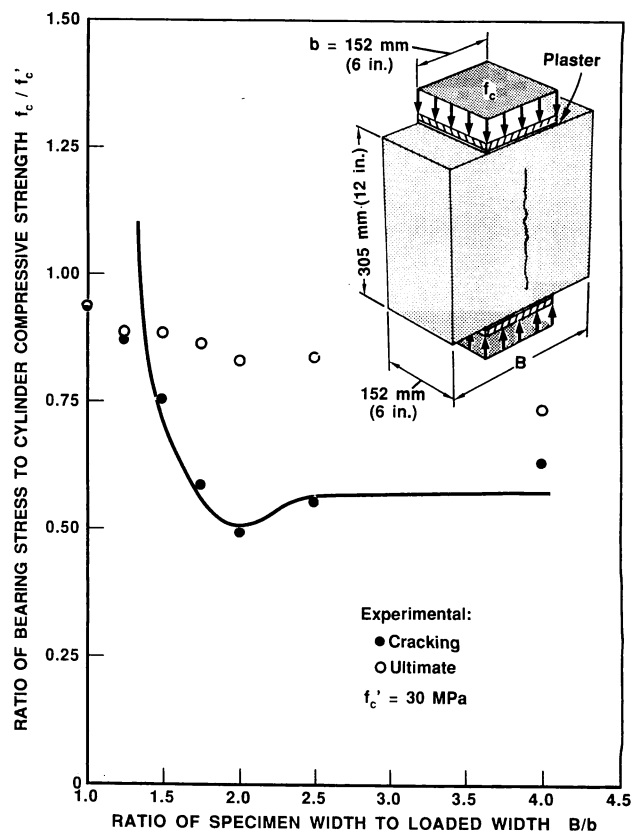


**Fig. 17—Simple tests to demonstrate the influence of transverse tension**

when the maximum tensile stress reached 3.3 MPa (1579 psi).

For these plane-stress specimens, the minimum bearing stress at cracking was approximately  $0.5f'_c$ , but in a pile cap the compressive stresses spread in two directions, reducing the transverse tension in any one direction. Chen<sup>16</sup> conducted a series of tests on variously sized concrete cylinders loaded in uniaxial compression through small round loading disks (double-punch test). In these tests the concrete cracked at a minimum bearing stress of  $1.5f'_c$ .

In the author's plane stress tests, the concrete continued to carry load after cracking (see Fig. 17), while in Chen's double-punch tests, failure was always coincident with cracking. In pile caps, the absence of reinforcement to control diagonal cracking allows the cracks that occur due to splitting of the struts to propagate quickly through the specimen. Depending on the geometry of the pile cap, the final kinematically feasible failure mechanism resembles either a one-way or two-way shear failure.

It has been suggested<sup>1</sup> that if the maximum bearing stress is less than some critical value, a splitting strut failure will be prevented. Examining the maximum bearing stress in those pile caps that had strut failures, it appears a limit on the maximum bearing stress of about  $1.0f'_c$  is reasonably conservative for pile caps (see Table 7). Note that if the pile cap capacities are predicted using the simple maximum bearing stress rule, the coefficients of variation are 10.9 and 4.8 percent for

the pile and column bearing stresses, respectively. For the same pile caps, the ACI 318 predictions of shear strength give a coefficient of variation of 23 percent.

### COMPARISON WITH CANADIAN CONCRETE CODE

The Canadian concrete code's shear-design rules, which make use of strut-and-tie models, were intended for plane structures such as corbels or deep beams; however, they are general enough that they can be applied to pile caps. The Canadian code requires that the concrete compressive stress in nodal zones of strut-and-tie models does not exceed  $0.85f'_c$  in nodal zones bounded by compressive struts,  $0.75f'_c$  in nodal zones anchoring only one tension tie, and  $0.60f'_c$  in nodal zones anchoring more than one tie. The Canadian code also requires that the necessary tension-tie reinforcement be effectively anchored to transfer the required tension to the nodal zones. Finally, the concrete compressive stress in struts must not exceed the crushing strength of the cracked concrete determined by considering the strain conditions in the vicinity of the strut. Further details can be found in Reference 6.

Table 8 compares the Canadian code's predicted strengths of the test specimens with the experimentally observed failure loads. For Pile Cap A, failure is predicted to occur when the longitudinal reinforcement yields. For all other pile caps, the limitation that the column bearing stress must not be greater than  $0.85 f'_c$  is critical.

The limitation on concrete compressive stress in the struts was not critical for the pile caps tested. However, the strength of shallower pile caps with flatter compression struts may be limited by the compression in the struts, since the strength of a strut tends to zero as the angle between strut-and-tie tends to zero. If a pile cap has very flat compression struts, then the internal force flow will be relatively uniform and a sectional force approach would be appropriate. Such a sectional force approach would assume the shear strength of a pile cap is proportional to the depth of concrete. For slender pile caps supported on numerous piles, the Canadian code allows designers to use a sectional force procedure similar to the ACI procedure.

### PILE LOAD DISTRIBUTION

Designers of pile caps usually assume a uniform distribution of load among piles. But studies<sup>17</sup> have shown that the load applied to a "rigidly" capped free-standing pile group is usually not uniformly distributed; in fact, the difference in load between two adjacent piles may be more than 100 percent. Assuming the pile loads are all equal implies that a pile cap has considerable flexibility. The results from this study indicate that this is not the case.

Prior to first cracking, the statically indeterminate test specimens were, within the precision of displacement measurements, perfectly rigid. The initial pile load distributions were proportional to the stiffnesses of the pseudo-piles. Very little cracking was observed in the

**Table 7 — Maximum bearing stresses as a function of the concrete cylinder strengths**

Pile Cap	Concrete strength $f'_c$ , MPa	Maximum pile load, kN	Maximum column load, kN	Ratio of pile bearing stress to concrete strength	Ratio of column bearing stress to concrete strength
C	27.1	1270	2892	1.49	1.19
D	30.3	1119	3222	1.18	1.18
E	41.1	1655	4709	1.28	1.27
F	30.3	1077	3026	1.13	1.11
				Mean = 1.27 COV* = 10.9%	Mean = 1.19 COV* = 4.8%

\*COV = coefficient of variation.  
1 MPa = 145 psi; 1 kN = 0.225 kip.

**Table 8 — Comparison of Canadian concrete code predictions and experimentally observed failure loads**

Pile Cap	Concrete strength $f'_c$ , MPa	Predicted load, kN	Experimental load, kN	Exp. Pred.
A	24.8	1735	1781	1.03
B	24.8	1897	2189	1.15
C	27.1	2073	2892	1.40
D	30.3	2318	3222	1.39
E	41.1	3144	4709	1.50
F	30.3	2318	3026	1.31

Mean = 1.30  
COV = 13.5%

1 MPa = 145 psi; 1 kN = 0.225 kip.

pile caps until after failure; as a result, there was little redistribution of the pile loads. Pile Caps A, B, and C, in which the reinforcement yielded, had on average about 13 percent redistribution of load between the short-direction and long-direction piles. The more heavily reinforced Pile Caps D, E, and F had only 5 percent redistribution from the short to long direction (see Table 4). In all specimens, the pile-load distribution at failure was far from uniform.

Before an indeterminate structure can be properly designed (using either strut-and-tie models or the ACI approach), the support reactions have to be determined by an analysis that reflects the behavior of the actual structure. For deep pile caps without shear reinforcement, an analysis that assumes the pile cap remains perfectly rigid is appropriate. The small amount of redistribution that may occur should be neglected.

### CONCLUDING REMARKS

Fig. 18 compares the experimentally observed failure loads of four test specimens with predictions from the ACI Building Code and the Canadian code strut-and-tie model approaches. It can be seen that the ACI Building Code fails to capture the trend of the experimental results. This is because the ACI Building Code predictions exaggerate the importance of the effective depth  $d$ , neglect the influence of the horizontal distribution of longitudinal reinforcement, and most importantly, neglect the influence of amount of longitudinal reinforcement. The ACI Building Code also incorrectly predicts that the missing "corner" pieces of plain concrete in Pile Cap F will greatly reduce the strength of this spec-

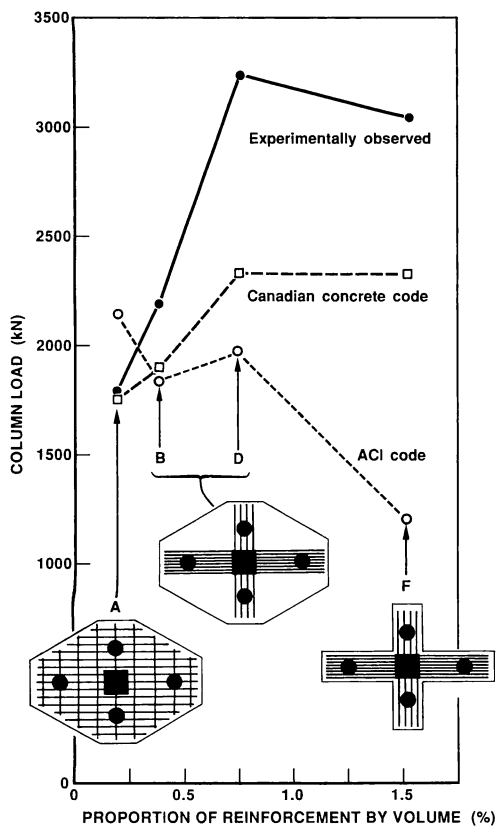


Fig. 18—Comparison of code predictions and experimentally observed failure loads for Pile Caps A, B, D, and E (1 kN = 0.225 kips)

imen, which is otherwise identical to Pile Cap D. The Canadian code, though conservative, reflects more accurately the trend of the experimental results.

The experimental observations have shown that, although ACI 318 treats pile caps similarly to two-way slabs, the behavior of deep pile caps is actually very different. Unlike lightly reinforced two-way slabs, which are very ductile because of flexural deformations, deep pile caps deform very little prior to failure. As a result, pile caps do not have the necessary flexibility to insure uniformity of pile loads at failure. Pile caps also do not behave as wide beams. Only a concentrated zone of concrete above the piles resists significant load. Further, plane sections do not remain plane in pile caps. Strut action, not beam action, is the predominant mechanism of shear resistance in pile caps.

Strut-and-tie truss models more accurately represent the behavior of deep pile caps. For example, strut-and-tie models correctly suggest that the load at which a lightly reinforced pile cap fails in two-way shear depends on the quantity of longitudinal reinforcement.

Compression struts in deep pile caps do not fail by crushing of the concrete. Failure occurs after a compression strut splits longitudinally due to the transverse tension caused by spreading of the compressive stresses. The maximum bearing stress is a good indicator of the likelihood of a strut splitting failure. For the pile caps tested, the maximum bearing stress at failure had a lower limit of about  $1.1f'_c$ . To prevent shear fail-

ures, the maximum bearing stress on deep pile caps should be limited to about  $1.0f'_c$ .

The shear strength of slender pile caps is proportional to the thickness of concrete. But the "shear strength" of deep pile caps with steep compression struts is better enhanced by increasing the bearing area of the concentrated loads rather than further increasing the depth of the pile cap.

## ACKNOWLEDGMENTS

The experimental work was performed in the Structures Laboratory of the Department of Civil Engineering at the University of Toronto. Support from the Natural Sciences and Engineering Research Council of Canada is gratefully acknowledged.

## REFERENCES

- Schlaich, Jörg; Schafer, Kurt; and Jennewein, Matthias, "Toward a Consistent Design of Reinforced Concrete Structures," *Journal*, Prestressed Concrete Institute, V. 32, No. 3, May-June 1987, pp. 74-150.
- Marti, Peter, "Basic Tools of Reinforced Concrete Beam Design," *ACI JOURNAL*, *Proceedings* V. 82, No. 1, Jan.-Feb. 1985, pp. 46-56.
- Cook, William D., and Mitchell, Denis, "Studies of Disturbed Regions Near Discontinuities in Reinforced Concrete Members," *ACI Structural Journal*, V. 85, No. 2, Mar.-Apr. 1988, pp. 206-216.
- Rogowsky, D. M., and MacGregor, J. G., "Design of Reinforced Concrete Beams," *Concrete International: Design and Construction*, V. 8, No. 8, Aug. 1986, pp. 49-58.
- "Design of Concrete Structures for Buildings," (CAN3 A23.3-M84), Canadian Standards Association, Rexdale, 1984, 281 pp.
- Collins, Michael P., and Mitchell, Denis, "Rational Approach to Shear Design—The 1984 Canadian Code Provisions," *ACI JOURNAL*, *Proceedings* V. 83, No. 6, Nov.-Dec. 1986, pp. 925-933.
- Rogowsky, David M.; MacGregor, James G.; and Ong, See Y., "Tests of Reinforced Concrete Deep Beams," *ACI JOURNAL*, *Proceedings* V. 83, No. 4, July-Aug. 1986, pp. 614-623.
- Lee, D., "An Experimental Investigation of the Effects of Detailing on the Shear Behaviour of Deep Beams," MSc thesis, University of Toronto, 1982, 179 pp.
- Blévet, J., and Frémy, R., "Semelles sur Pieux," *Annales*, Institut Technique du Bâtiment et des Travaux Publics (Paris), V. 20, No. 230, Feb. 1967, pp. 223-295.
- Clarke, J. L., "Behaviour and Design of Pile Caps with Four Piles," *Technical Report* No. 42.489, Cement and Concrete Association, London, Nov. 1973, 19 pp.
- Sabnis, Gajanan M., and Gogate, Anand B., "Investigation of Thick Slabs (Pile Cap) Behavior," *ACI JOURNAL*, *Proceedings* V. 81, No. 1, Jan.-Feb. 1984, pp. 35-39.
- Adebar, P., "The Behaviour of Pile Caps: An Experimental Investigation," MSc thesis, Department of Civil Engineering, University of Toronto, Jan. 1987, 135 pp.
- Kuchma, D. A., "Design Using the Strut and Tie Model: Tests of Large-Scale Pile Caps," MSc thesis, Department of Civil Engineering, University of Toronto, Apr. 1989, 137 pp.
- Park, Robert, and Paulay, Thomas, *Reinforced Concrete Structures*, Wiley-Interscience, New York, 1975, 769 pp.
- Vecchio, Frank J., and Collins, Michael P., "Modified Compression-Field Theory for Reinforced Concrete Elements Subjected to Shear," *ACI JOURNAL*, *Proceedings* V. 83, No. 2, Mar.-Apr. 1986, pp. 219-231.
- Chen, W. F., and Trumbauer, B. E., "Double-Punch Tests and Tensile Strength of Concrete," *Journal of Materials*, V. 7, No. 2, June 1972, pp. 148-154.
- Beredugo, Y. O., "Experimental Study of the Load Distribution in Pile Groups in Sand," *Canadian Geotechnical Journal* (Ottawa), V. 3, 1966, pp. 145-166.
- Chen, Wai-Fah, "Double Punch Test for Tensile Strength of Concrete," *ACI JOURNAL*, *Proceedings* V. 67, No. 12, Dec. 1970, pp. 933-995.